Transport and mixing in traveling waves

Jeffrey B. Weiss
National Center for Atmospheric Research, P.O. Box 3000, Boulder, Colorado 80307

(Received 28 August 1990; accepted 12 November 1990)

An iterated map is constructed that captures the essential features of particle trajectories in a class of quasiperiodic traveling waves: large-amplitude single-frequency traveling waves with two-dimensional structure perturbed by a wave with a second frequency. The map provides an efficient method for numerical calculation of the transport and mixing properties of such waves, and is used here to study the properties of a chaotic separatrix layer. It is found that the average position increases linearly with time indicating the existence of a well-defined transport velocity. The transport velocity grows faster than linearly as the perturbation parameter k increases. The mixing takes the form of anomalous diffusion where the mean-square deviation of position grows as t^{ν}, with $\nu > 1$. The data is consistent with the diffusion exponent ν growing linearly with k.

I. INTRODUCTION

Traveling waves are a common feature of many fluid systems, including the atmosphere,[1,2] ocean,[3] and laboratory flows.[4–8] The presence of these waves can have a profound influence on the transport and mixing properties of a fluid, properties which are important in many physical situations. In the atmosphere, for example, the transport and mixing of various chemical constituents is a key factor in several major problems: the transport and mixing of sulfur dioxide and chlorofluorocarbons are related to acid rain and ozone depletion, respectively. Understanding the role of traveling waves in producing transport and mixing is of interest in a variety of situations.

In many cases the traveling waves of interest have an approximate two-dimensional structure, allowing use of two-dimensional fluid dynamics. In the atmosphere, the rapid rotation of the Earth results in large-scale Rossby waves whose structure lies largely in the horizontal plane,[2] while in laboratory convection the structure is in a vertical plane.[4–6] In either case the two-dimensional structure, together with the assumption of incompressibility, allows the flow to be described in terms of a streamfunction $\Psi(x,y,t)$, where (x,y) is the plane containing the structure of the wave. The trajectories of small parcels of fluid, henceforth called "fluid particles," are obtained from the streamfunction by integrating the equations of motion,

$$\frac{dx}{dt} = \frac{\partial\Psi(x,y,t)}{\partial y}, \quad \frac{dy}{dt} = -\frac{\partial\Psi(x,y,t)}{\partial x}. \tag{1}$$

The above equation does not include molecular diffusion. While molecular diffusion does introduce some additional effects, they are for the most part small and will be largely ignored.

Questions of transport and mixing revolve around the motion of fluid particles. The term transport refers to the motion of groups of fluid particles from one region to another. Quantitatively, we shall measure transport by the motion of the average position of an ensemble of particles, $\langle x \rangle$. By the term mixing we shall refer to the spreading of fluid particles originally concentrated close together. As the fluid particles spread, they mix with the surrounding fluid. One quantitative measure of such spreading is the growth of the mean-square deviation of particle positions as a function of time, $M(t) = \langle (x - \langle x \rangle)^2 \rangle$.

Studies of transport and mixing in two-dimensional incompressible fluids benefit from the correspondence between two-dimensional incompressible fluid flow and Hamiltonian dynamics.[9] The equations of motion (1) are identical to Hamilton's equations of motion, with the streamfunction corresponding to the Hamiltonian, and the particle trajectories in physical space corresponding to trajectories in phase space. A fluid with a time-independent streamfunction is thus an integrable Hamiltonian system, and the particle trajectories are then regular (periodic or quasiperiodic). A time-periodic streamfunction may be nonintegrable, giving rise to chaotic particle trajectories. We shall be particularly interested in the effect such chaotic trajectories have on the transport and mixing properties of traveling waves.

A preliminary understanding of transport and mixing by traveling waves has been obtained by previous studies on waves.[10–18] Such work includes both theoretical studies of idealized waves, and experimental studies of convective waves in binary fluids and nematic liquid crystals. The next several paragraphs provide a summary of this understanding.

Single-frequency traveling waves with infinitesimal amplitude transport energy and momentum but not particles. As the wave amplitude increases, the phenomenon of Stokes' drift appears: particles drift in the direction of the phase velocity of the wave, with the drift speed proportional to the square of the wave amplitude. At large wave amplitudes particle trapping occurs, where, in certain regions of the fluid, particles are carried with the wave at the wave's phase speed. The phenomenon of particle trapping can occur whenever the streamfunction, in a frame comoving with the wave, has the form of a wave superposed on a mean flow. Particle trapping then occurs when the wave amplitude is greater than some threshold amplitude. The value of the threshold depends on the structure of the wave, but, for the cases studied, has always been found to be an $O(1)$ number times the velocity of the mean flow.

 0899-8213/91/051379-06$02.00

Two-dimensional single-frequency traveling waves have a time-independent streamfunction in a frame comoving with the wave. Above the trapping threshold, the fluid is divided into regions of trapped particles, which are carried with the wave as it propagates, and free particles, which flow backward with respect to the wave. These regions are separated by a special trajectory, a separatrix, which, in a frame comoving with the wave, is homoclinic to a fixed point lying in the interior of the fluid. In studies of waves using free-slip boundary conditions, the regions may be separated by a trajectory that is heteroclinic to a pair of fixed points lying on the boundary. However, since the fixed points are in a moving frame, they can only lie on the boundary if free-slip boundary conditions are used; realistic boundary conditions force the fixed points into the interior of the fluid. This distinction is not thought to greatly affect the transport and mixing properties of the wave. The streamfunction of a typical traveling wave in a comoving frame is shown in Fig. 1.

In an infinite wave train, trapped particles only become free through the action of molecular diffusion, at which point they are deposited at a location which may be very far from their origin. Similarly, free particles may become trapped and carried great distances by diffusing into the trapping region of the flow. Although the mixing produced by the combination of molecular diffusion and trapping and untrapping events is larger than that produced by molecular diffusion alone, it is still small compared to that produced by the quasiperiodic traveling waves discussed below.

If a second frequency is present in the wave then the possibility of chaotic particle trajectories arises. In this case, the separatrix between the trapped and free regions breaks, resulting in a chaotic region bounded by Kolmogorov–Arnold–Moser (KAM) curves. Particles in such a region chaotically alternate between being trapped and carried with the wave, and being free and drifting backward relative to the wave. The net result is both long-range transport and enhanced mixing. Further, the mixing takes the form of anomalous diffusion, where $M(t)$ grows as t^{ν}, with $\nu > 1$.

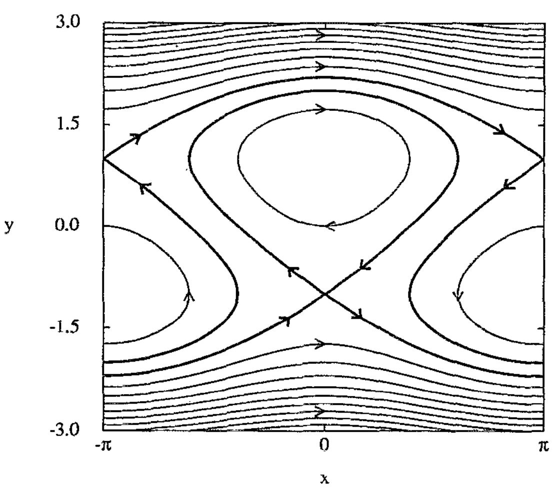

FIG. 1. Traveling wave flow given by Eq. (2). Heavy lines denote homoclinic trajectories.

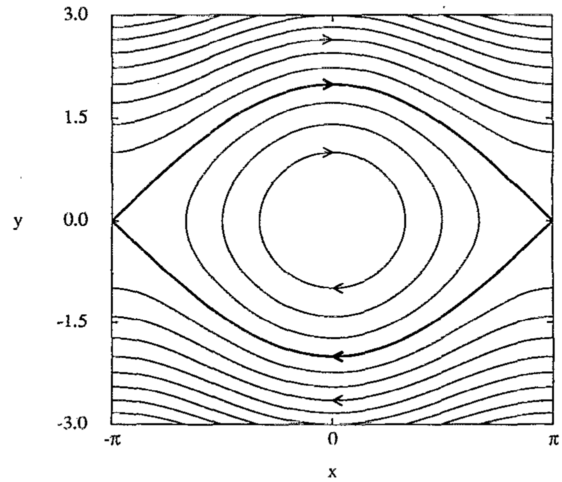

FIG. 2. Pendulum flow. Heavy lines denote homoclinic trajectories.

Thus, previous work has provided a qualitative picture of the transport and mixing properties of waves. It is of great interest, however, to understand how these properties depend quantitatively on the parameters describing the wave. Unfortunately, integrating the equations of motion for particle trajectories, Eq. (1), can be very costly, making numerical studies of parameter dependence impractical. The aim of this paper is to construct an iterated mapping which can be used to calculate particle trajectories efficiently, providing a tool with which to study the parameter dependence of transport and mixing properties of waves.

Perhaps the most studied chaotic Hamiltonian system is the periodically forced pendulum. The unforced pendulum Hamiltonian, shown in Fig. 2, has many similarities to the single-frequency traveling wave we consider here. First, both are periodic in one direction; thus phase space may be considered to be a cylinder. Comparing Figs. 1 and 2 one sees that both the pendulum and traveling wave have trapped regions where trajectories circle a fixed point, and free regions where trajectories circle the phase space cylinder. The major difference between the two is that in the pendulum there are trajectories circling the phase space cylinder in either direction, while in the traveling wave these trajectories only travel in one direction. This property of traveling waves is due to the fact that in a fixed reference frame the trapped region moves with the phase velocity of the wave, while the free region is left behind; thus in a comoving frame all trajectories in the free region must flow in the direction opposite the phase velocity.

One tool that has proved extremely useful in understanding the properties of the periodically forced pendulum, and near-integrable Hamiltonians in general, is the standard map.[19,20] The standard map displays behavior typical of near-integrable Hamiltonian systems: chaotic and regular regions, KAM curves, cantori, etc. One major advantage of studying the standard map rather than a set of ordinary differential equations is that it is much faster to numerically iterate a map than to integrate differential equations numerically. Because of the differences between the pendulum flow and the traveling wave flow, however, the standard map does not capture the essential features of traveling waves.

In Sec. II we shall construct an iterated map analogous to the standard map which does capture the essential features of traveling waves. This map, which we call the traveling wave map, provides an efficient tool for numerically calculating the transport and mixing properties of two-dimensional large-amplitude quasiperiodic traveling waves. In Sec. III the results of some numerical calculations of transport and mixing in the traveling wave map are presented.

II. THE TRAVELING WAVE MAP

One method of obtaining the standard map is to start with the flow for the unperturbed pendulum and then add a periodic delta-function perturbation. Analogously, to obtain the traveling wave map we start with a flow that captures the essential features of large-amplitude single-frequency traveling waves with two-dimensional structure. These features are known from experimental and theoretical studies of traveling waves in various physical systems.[10-18]

Since we are concerned with incompressible waves with two-dimensional structure, the flow must be Hamiltonian with one degree of freedom. In a frame comoving with the single-frequency wave the flow is steady, so we seek a time-independent streamfunction. The flow must be periodic in the direction along the wave; the phase space is thus a cylinder. The flow should contain regions of trapped particles, where the trajectories circle a fixed point, and regions of free particles, where trajectories circle the phase space cylinder in a single direction. Waves with positive phase velocities have free trajectories circling the cylinder in the negative direction, and vice versa. Finally, the free and trapped regions should be separated by a trajectory homoclinic to a fixed point lying in the interior of the flow.

A simple flow which satisfies the above requirements is

$$\frac{dx}{dt} = y^2 - 1, \quad \frac{dy}{dt} = -\sin x, \tag{2}$$

corresponding to a traveling wave moving in the negative x direction. Equation (2) describes a wave with arbitrary phase speed in a comoving frame, and is shown in Fig. 1. Because of the symmetry $x \to x + \pi$, $y \to -y$, the flow contains two trapped regions centered around stable fixed points at $(x,y) = (0,1), (\pi, -1)$. The trapped regions are separated from free regions by trajectories homoclinic to the unstable fixed points at $(x,y) = (0,-1), (\pi,1)$. The Hamiltonian, or streamfunction, of the flow is

$$\Psi_0(x,y) = (y^3/3) - y - \cos x. \tag{3}$$

Note that the flow (2) differs from the pendulum flow only in the dx/dt equation, where $dx/dt = y$. The quadratic dependence on y results from requiring dx/dt to have the same sign at both large positive and large negative y.

We construct the traveling wave map from the above flow by following the construction of the standard map from the pendulum. The streamfunction (3) is perturbed by adding the time-periodic streamfunction

$$\Psi_1(x,y,t) = \cos(x)\left(1 - \sum_{n=-\infty}^{\infty} k\delta(t - nk^+)\right), \tag{4}$$

where the argument of the delta function means the impulse occurs just after $t = nk$. The perturbation parameter k is both the period of the perturbation and the strength of the delta function. The resulting flow is

$$\begin{aligned} \frac{dx}{dt} &= y^2 - 1, \\ \frac{dy}{dt} &= -\sin(x) \sum_{n=-\infty}^{\infty} k\delta(t - nk^+). \end{aligned} \tag{5}$$

To obtain the traveling wave map one now integrates over one period of the perturbation, resulting in the traveling wave map:

$$\begin{aligned} x_{n+1} &= x_n + k(y_{n+1}^2 - 1), \\ y_{n+1} &= y_n - k \sin x_n, \end{aligned} \tag{6}$$

where $(x_n, y_n) = [x(t), y(t)]|_{t=nk}$. The traveling wave map (6) approaches the pure traveling wave flow (2) as $k \to 0$ in the sense that

$$\begin{aligned} \lim_{\substack{k\to 0 \\ nk=t}} \frac{x_{n+1} - x_n}{k} &= \lim_{k \to 0} \frac{x(t+k) - x(t)}{k} \\ &= \frac{dx(t)}{dt} = y(t)^2 - 1, \end{aligned} \tag{7}$$

and similarly for the y equation.

Figures 3 and 4 depict the traveling wave map for $k = 0.1$ and $k = 0.4$, respectively. Each figure results from 26 initial conditions iterated 500 times, and at each iteration x is mapped back to $(-\pi, \pi)$. The blank regions can be obtained by the symmetry $x \to x + \pi$, $y \to -y$. At $k = 0.1$ the map appears almost identical to the unperturbed traveling wave (Fig. 1). As k is increased to 0.4 the typical features of chaotic Hamiltonian systems appear; island chains and chaotic layers become visible. Of particular importance is that the separatrix between the free and trapped regions of the wave breaks, resulting in a chaotic separatrix layer.

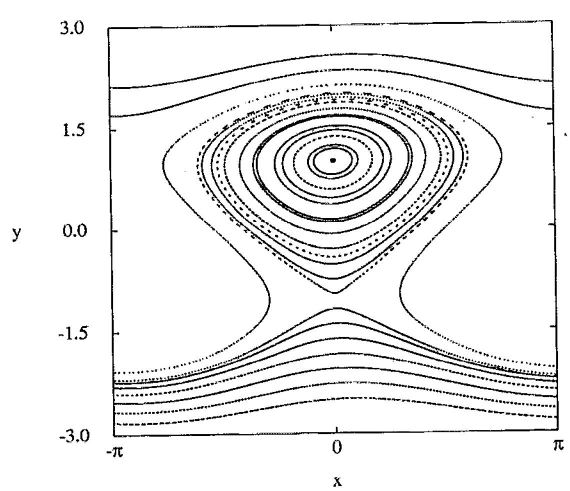

FIG. 3. Traveling wave map for $k = 0.1$ with x mapped back to $(-\pi, \pi)$.

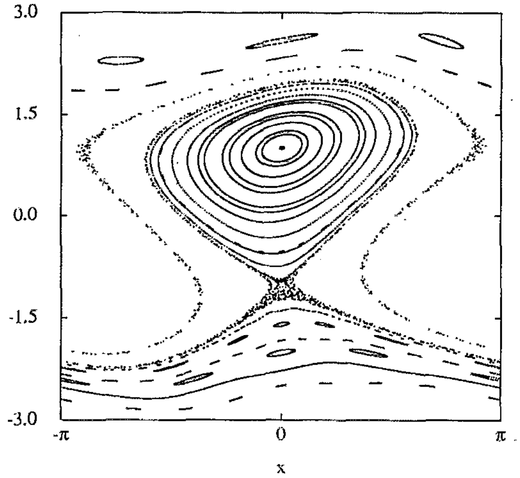

FIG. 4. Traveling wave map for $k = 0.4$ with x mapped back to $(-\pi,\pi)$.

These features are present at all nonzero k, but for small k are too small to see without magnifying the appropriate regions of phase space. As k is increased further the chaotic regions grow until they merge and fill all of phase space. In what follows we shall only be concerned with relatively small values of k.

III. TRANSPORT AND MIXING IN THE TRAVELING WAVE MAP

The perturbation of a single-frequency traveling wave by a second frequency can cause the fluid to break into three types of regions: trapped regions in which particles are perpetually carried with the wave, free regions in which particles are perpetually left behind by the wave, and chaotic separatrix layers between the two in which particles alternate between episodes of trapped and free behavior. These regions are separated by KAM curves that, except for the effects of molecular diffusion, prevent the exchange of particles between regions. The trapped and free regions are similar to corresponding regions in single-frequency traveling waves. In the remainder of this paper we shall focus on particle behavior in a chaotic separatrix layer, a region which is not present in a single-frequency wave.

Particles in the separatrix layer are restricted in their motion transverse to the wave, the y direction, due to the presence of KAM curves. Large-scale motions along the wave, in the x direction, are possible because the separatrix layer wraps around the phase space cylinder, and thus extends from $x = -\infty$ to $x = +\infty$. It is the transport and mixing in the x direction which will occupy our attention.

The properties of the chaotic separatrix layer were investigated through a series of numerical experiments. Each experiment started with an ensemble of 1000 initial conditions chosen randomly along the line $x = 0$, with y inside the chaotic region. Trajectories were then calculated for 10^6 iterations of the traveling wave map (6), from which the average position $\langle x \rangle$ and mean-square deviation of position M were determined.

Although all initial conditions were started within the outermost boundaries of the chaotic region, some may actually be inside islands and thus be perpetually trapped or free. To exclude these particles, ensemble averages only included particles displaying at least one trapped and one free episode.

Numerical experiments were carried out for k ranging from 0.2 to 0.4 in steps of 0.05. As k becomes smaller, the duration of trapped and free episodes, measured in number of iterations, becomes longer. For $k < 0.2$, it is felt that 10^6 iterations are not sufficient to adequately characterize the chaotic dynamics. At selected values of k, two identical experiments were run using independent ensembles of initial conditions, thus giving an estimate of the uncertainty due to finite sample size.

The average position as a function of iteration number for $k = 0.3$ is plotted in Fig. 5. One sees that $\langle x \rangle$ grows linearly with time, indicating the existence of a well-defined transport velocity v. Since time is given by kn, v is defined by the slope of the least-squares fit divided by k.

The mean-square deviation M is shown for $k = 0.3$ in Fig. 6. The approximately linear growth of M on a log–log plot indicates that $M(t) \sim t^{\nu}$. The diffusion exponent ν is the slope of a least-squares fit of $\log(M)$ vs $\log(n)$. Note that the variation of M about the fit is noticeably larger than that of $\langle x \rangle$.

The behavior shown in Figs. 5 and 6 is typical of the range of k studied. We find a well-defined transport velocity $v(k)$, and a less well-defined diffusion exponent $\nu(k)$ due to the variation of M about its least-squares fit.

Figure 7 shows $v(k)$ for the range of k studied. One sees that v grows monotonically with k, with nonlinear growth apparent at the two largest values of k. Thus, waves corresponding to larger values of k are more effective at transporting fluid particles in the chaotic separatrix layer downstream, in the frame of the wave.

Figure 8 shows $\nu(k)$ vs k. The variation in the independent ensembles at the same k is larger than that for v. This

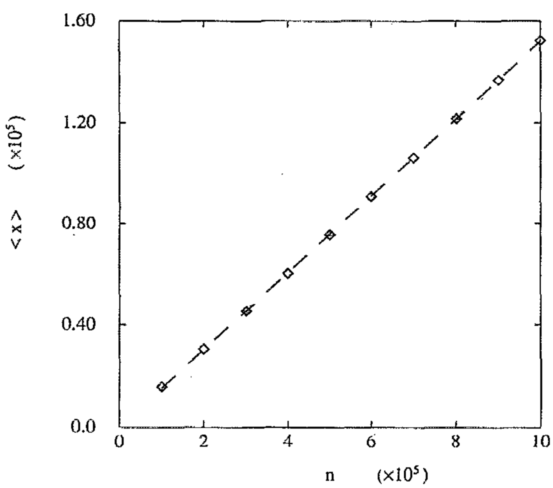

FIG. 5. Average position $\langle x \rangle$ vs n for $k = 0.3$. Diamonds represent data calculated with the traveling wave map, and the dashed line is a least-squares fit.

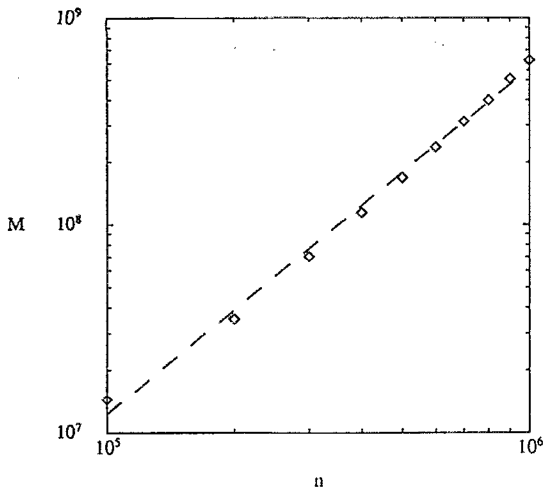

FIG. 6. Mean-square deviation of position M vs n for $k = 0.3$. Diamonds represent data calculated with the traveling wave map, and the dashed line is a least-squares fit.

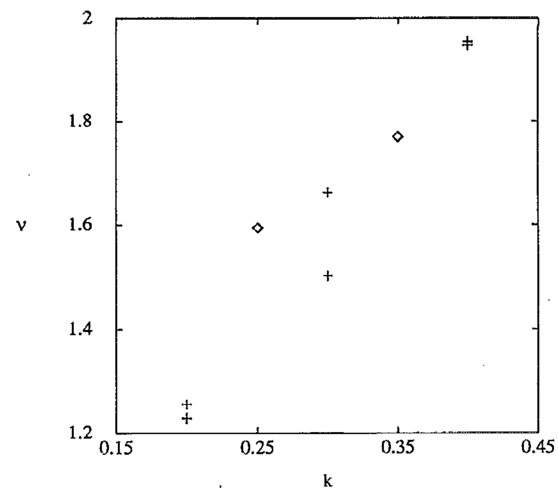

FIG. 8. Diffusion exponent ν vs k. Diamonds represent values of k for which one ensemble of initial conditions was used. Plus signs indicate values of k where two ensembles were used.

indicates that larger ensembles, and perhaps longer trajectories, would allow a more precise determination of ν. The data is consistent with linear growth of ν with k, although more data are needed to be certain. One interpretation of $\nu > 1$ is in terms of a time-dependent diffusion coefficient. Thus, as time progresses, the chaotic separatrix layer of quasiperiodic waves becomes more and more efficient at mixing the fluid in the layer. Furthermore, as k increases, the diffusion coefficient grows faster with time.

IV. DISCUSSION

In this paper we have constructed an iterated mapping that allows the efficient calculation of the transport and mixing properties of a class of waves. The map captures the essential features of large-amplitude single-frequency traveling waves with two-dimensional structure, which are perturbed by a two-dimensional wave with a second frequency. At sufficiently large amplitude, such unperturbed waves contain a homoclinic connection which may break under the perturbation, resulting in chaotic particle trajectories. The behavior of these chaotic trajectories is well represented by the traveling wave map.

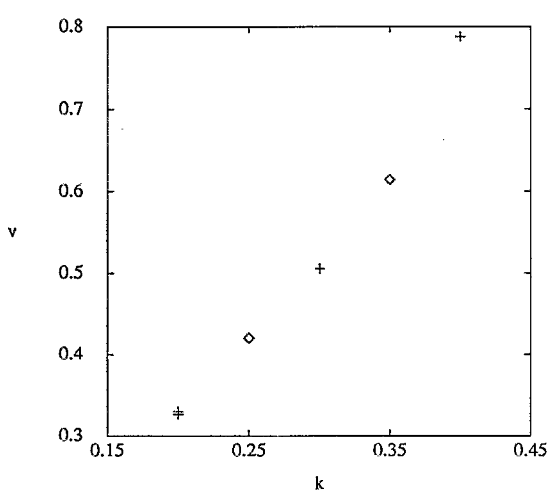

FIG. 7. Transport velocity v vs k. Diamonds represent values of k for which one ensemble of initial conditions was used. Plus signs indicate values of k where two ensembles were used. Where the two ensembles give very similar results the two plus signs overlap and appear as one.

We have used the traveling wave map to investigate the transport and mixing properties of the chaotic trajectories. We find that as the amplitude of the perturbation increases, the transport velocity increases faster than linearly, while the diffusion exponent increases in a manner consistent with linear growth. The finding that $\nu > 1$ is consistent with previous studies showing anomalous diffusion by traveling waves.[16,18] The calculations presented here, however, are, to our knowledge, the first results indicating the dependence of the transport velocity and diffusion exponent on a parameter of the wave.

We have been concerned in this paper with the transport and mixing properties resulting from the complex structures present in a chaotic phase space. The addition of molecular diffusion will smear out the fine details of these structures, allowing trajectories to eventually cross KAM curves and pass more easily through cantori. We expect that in the presence of molecular diffusion, the traveling wave map captures the dynamics for only a finite time. The cutoff time, which is determined by the time scale for molecular diffusion to carry a particle across a significant fraction of the chaotic layer, is, for small molecular diffusion, quite large.

The traveling wave map constructed here allows an exploration of the manner in which the transport and mixing properties depend on the parameters in an idealized wave. While such details as the exact shapes of the homoclinic orbits and the boundary of the chaotic regions will depend on the details of the wave, the phenomenon of enhanced transport and mixing through the trapping and untrapping of fluid particles is quite general. Such trapping and untrapping will occur in any flow with a broken homoclinic connection.

As parameters of a wave are varied, the structures in phase space are altered, resulting in different transport and mixing properties. The traveling wave map provides an efficient tool for understanding how these properties are affected by the structures in phase space. By then investigating how the variation of parameters in a realistic wave affects the structures in phase space, one could determine how a given realistic wave affects the transport and mixing properties without an extensive calculation of trajectories.

For example, we have found that as k increases, the width of the chaotic layer increases, accompanied by an increase in both the transport velocity and the diffusion exponent. This leads us to conjecture that the variation of a parameter in a realistic wave which results in a wider chaotic layer would have a similar effect. One must be careful, however, since it may not be just the width of the chaotic layer that is important here. Such things as the sizes of gaps in the cantori, or the density of island chains in the chaotic layer, may prove to be dominant. It is unknown whether such things scale simply with the width of the chaotic layer. Nonetheless, once it is understood how structures in phase space affect transport and mixing, it should be much simpler to characterize the transport and mixing properties of a variety of realistic waves.

ACKNOWLEDGMENTS

I would like to thank Edgar Knobloch for many interesting and helpful discussions.

This work was supported in part by a grant from Cray Research, Inc. The National Center for Atmospheric Research is sponsored by the National Science Foundation.

[1] J. T. Houghton, *The Physics of Atmospheres* (Cambridge U.P., Cambridge, 1986).
[2] J. Pedlosky, *Geophysical Fluid Dynamics* (Springer, New York, 1987).
[3] P. H. LeBlond and L. A. Mysak, *Waves in the Ocean* (Elsevier/North-Holland, New York, 1980).
[4] R. W. Walden, P. Kolodner, A. Passner, and C. M. Surko, Phys. Rev. Lett. **55**, 496 (1985).
[5] E. Moses and V. Steinberg, Phys. Rev. A **34**, 693 (1986).
[6] R. Heinrichs, G. Ahlers, and D. S. Cannell, Phys. Rev. A **35**, 2761 (1987).
[7] H. Niino and N. Misawa, J. Atmos. Sci. **41**, 1992 (1984).
[8] J. Sommeria, S. D. Meyers, and H. L. Swinney, Nature **337**, 58 (1989).
[9] H. Aref, Annu. Rev. Fluid Mech. **15**, 345 (1983).
[10] E. Knobloch and J. B. Weiss, in *The Internal Solar Angular Velocity*, edited by B. R. Durney and S. Sofia (Reidel, Worwell, MA, 1987).
[11] E. Knobloch and J. B. Weiss, Phys. Rev. A **36**, 1522 (1987).
[12] T. H. Solomon and J. P. Gollub, Phys. Rev. A **38**, 6280 (1988).
[13] E. Moses and V. Steinberg, Phys. Rev. Lett. **60**, 2030 (1988).
[14] D. S. Broomhead and S. C. Ryrie, Nonlinearity **1**, 409 (1988).
[15] S. J. Linz, M. Lücke, H. W. Müller, and J. Niederländer, Phys. Rev. A **38**, 5727 (1988).
[16] J. B. Weiss and E. Knobloch, Phys. Rev. A **40**, 2579 (1989).
[17] A. Joets and R. Ribotta, Europhys. Lett. **10**, 721 (1989).
[18] S. M. Cox, P. G. Drazin, S. C. Ryrie, and K. Slater, J. Fluid Mech. **214**, 517 (1990).
[19] A. J. Lichtenberg and M. A. Lieberman, *Regular and Stochastic Motion* (Springer, New York, 1983).
[20] R. S. Mackay and J. D. Meiss, *Hamiltonian Dynamical Systems* (Hilger, Bristol, 1987).